Available online at www.sciencedirect.com
ScienceDirect
Cold Regions Science and Technology 52 (2008) 355–370
cold regions science and technology
www.elsevier.com/locate/coldregions

Impact of snow cover on soil temperature and its simulation in a boreal aspen forest

Yinsuo Zhang [a,*], Shusen Wang [a], Alan G. Barr [b], T.A. Black [c]

[a] Canada Center for Remote Sensing, Natural Resources Canada, Ottawa, Ontario, Canada K1A 0Y7
[b] Climate Research Division, Environment Canada, Saskatoon, SK, Canada
[c] Faculty of Land and Food Systems, University of British Columbia, Vancouver, BC, Canada V6T 1Z4

Received 6 March 2007; accepted 7 July 2007

Abstract

Snow cover has low thermal conductivity and high albedo, which have large impacts on the soil thermal regime and microclimate. Accurate simulations of snow and soil processes are critical to ecosystem and climate modelling. In this study, we developed a detailed snow and soil scheme in an ecosystem model EALCO to (1) improve the simulations of snow and soil thermal regimes and (2) investigate the effects of different model configurations and parameterizations including snow and soil layering resolutions, fractional snow cover parameterization, water table and total soil column depths, and the inclusion/exclusion of a surface organic layer and unfrozen water in frozen soil. The model includes dynamic layering of snow, user-adjustable layering of soil, snow cover compaction and destructive metamorphisms, implicit solutions of the soil heat and water transfer equations using a finite difference method, distinct parameterizations of the surface organic layer and unfrozen water in frozen soil. The model was tested using nine years (1994–2002) of winter field measurements obtained in a boreal aspen forest. The tested variables included snow depth, snow temperature, soil heat flux, and soil temperatures at various depths. The results showed that the model well reproduced the snow and soil thermal regimes and their interactions observed at the site. The results also indicated that the simulation of snow cover duration was affected by the snow layering resolution and fractional snow cover parameterization. The simulation of soil temperature was affected by the soil layering resolution, the depths of water table and soil column, and the inclusion of a soil organic layer. Inclusion of unfrozen water in frozen soil was found to have only a small effect on soil temperature simulation at this site.
© 2007 Elsevier B.V. All rights reserved.

Keywords: Snow simulation; Thermal regime; Soil moisture; Frozen soil; EALCO

1. Introduction

During the 20th century, air temperature increased at a higher rate in the northern high latitudes than the global mean (McCarthy et al., 2001). Most global climate models (GCMs) project that this trend will continue in the 21st century, with more warming in winter than summer (McCarthy et al., 2001). Boreal forests in the region occupy about 21% of the earth's forested land surface. They contain 13% of the global carbon (C) stored in biomass (Whittaker and Likins, 1975) and 43% of the C stored in soil (Schlesinger, 1991). This large C stock could have a significant impact on atmospheric greenhouse gas concentration if the ecosystem C balance

* Corresponding author. Current address: Department of Geography & Environmental Studies, Carleton University, Rm. B349 Loeb Building, 1125 Colonel By Drive, Ottawa, Ontario, Canada K1S 5B6. Tel.: +613 520 2600x8799; fax: +613 520 4301.
E-mail address: yinsuo_zhang@carleton.ca (Y. Zhang).

0165-232X/$ - see front matter © 2007 Elsevier B.V. All rights reserved.
doi:10.1016/j.coldregions.2007.07.001

changes with climate change. Much effort has been made during the last decade to study the boreal forest and climate interactions through field measurements (e.g., Sellers et al., 1997) and modeling (e.g., Amthor et al., 2001). Compared to growing season processes, investigations of winter processes have received much less attention, although several recent studies addressed the snow cover, surface albedo and hydrological processes in boreal forests during winter (e.g. Viterbo and Betts, 1999; Betts, 2000; Essery et al. 2003; Stähli and Gustafsson, 2006). This is partially due to the difficulties in conducting field measurements and uncertainties in modeling the physical and ecosystem processes in winter. The C release from ecosystem respiration in winter can be a significant part of the annual C balance in boreal forest ecosystems. For example, the results in several boreal coniferous forests by Winston et al. (1997) showed that the C release from soil during the winter season was 40–55 g C m^{-2}, while Goulden et al. (1998) reported that the annual net ecosystem C exchange in a boreal old black spruce forest ranged from a source of 70 ± 50 g C m^{-2} to a sink of 10 ± 50 g C m^{-2}. At a southern boreal black spruce stand, winter (October–March) losses of C were 56%, 49%, and 83% of growing season (April–September) C uptake during the years 2000, 2001, and 2002, respectively (Black et al. 2005). Goulden et al. (1998) further indicated that the winter C release from boreal forests could become more important under climate warming due to increases of soil temperature and soil thaw.

Soil and plant C processes in winter are largely controlled by the soil temperature. In the boreal forest, snow covers the ground for about half of the year, with large interannual variability. With its high albedo, low thermal conductivity, large energy requirement for melting, and significant soil water input during melting, the snowpack causes the surface energy balance and soil microclimate to be fundamentally different in winter than summer. The effect of snow cover on soil temperature and ecology has been observed in several experimental studies. For example, snow removal in a high latitude maple tree stand caused more than 10 °C decrease in soil temperature, which resulted in severe physiological responses including increased canopy dieback and earlier leaf senescence in the subsequent growing season (Pilon et al. 1994). Contrasting to the hypothesis that future climate warming will likely cause warmer soil (e.g., Goulden et al., 1998), Groffman et al. (2001) projected a 'colder soils in a warmer world' scenario in snow-covered seasons based on their experimental results, due to the possible reduction of snowpack during warming. However, field experiments to study the interaction of snow cover and soil temperature can only test limited scenarios while future climate change may cause complex variations in snow cover. Numerical modeling is thus considered as an effective alternative for such studies (Yin and Arp, 1993; Levine and Knox, 1997; Ling and Zhang, 2004).

Needs for improved snow simulations have frequently been emphasized in recent modelling studies. In the model intercomparison studies by Slater et al. (2001) and by Nijssen et al. (2003), which involved 21 land surface models, it was found that the modeled snow depth and snow water equivalent (SWE) differed markedly due to differences in parameterizations of snow albedo, snow melting and sublimation, snow cover fraction, snow thermal properties, and the snow layering modelling schemes. Loth and Graf (1998) indicated that climate models need a multi-layer snow scheme in order to improve the energy exchange simulations in the snow-atmosphere and snow-soil interfaces and the soil thaw/freeze cycles. The inclusion of liquid water storage and transfer, densification due to compaction, destructive metamorphisms and melting were also found to be important in snow simulations (Kongoli and Bland, 2000; Gusev and Nasonova, 2003; Essery and Etchevers, 2004).

The number of vertical soil layers included in the current climate and ecosystem models differs widely. The single layer model is computational efficient, but may not represent the soil temperature and moisture regimes accurately. A multi-layer model can better simulate the vertical profiles of soil moisture and temperature. Model resolution in soil layering is particularly important in simulating the soil freeze/thaw cycles in cold regions (Slater et al., 2001; Luo et al. 2003). Due to the large amount of energy required in freezing/thawing, the use of thick soil layers could remarkably delay the modelled response time of soil freeze/thaw. However, increasing the soil layering resolution increases computing time and also requires more parameters representing the thermal and hydraulic characteristics of each layer. The results from the model intercomparison studies of Luo et al. (2003) and Amthor et al. (2001) implied that a finer vertical resolution is preferred to accurately simulate the soil temperature and moisture profiles. However, the question still remains as to how and to what extent soil layering resolution affects thaw/freeze and temperature simulations of the snow and soil.

The inclusion of unfrozen water in frozen soils (below 0 °C) could affect the soil temperature simulation by altering the soil thermal properties and has been emphasized by several modeling studies in permafrost regions (Li and Koike, 2003; Ling and Zhang, 2004). Although more and more climate and hydrological models have tended to include the unfrozen water parameterization (e.g. Cox et al. 1999; Niu and Yang, 2006), its influence on the soil temperature simulation in boreal forest regions has been rarely tested.

A surface organic layer is frequently present in boreal forest ecosystems. Due to its low thermal conductivity and high hydraulic conductivity, the surface organic layer significantly changes the rate of energy and water transfer between the soil and the atmosphere, and thus modifies the soil temperature and moisture profiles. Distinct parameterization of the surface organic layer has been recommended by several field and modeling studies (e.g., Bhatti et al., 2000; Ogée and Brunet, 2001), but its influence on winter soil temperature has not been tested.

In this paper, we describe the development of a detailed snow and soil scheme in the ecosystem model EALCO (Ecological Assimilation of Land and Climate Observations). The scheme includes dynamic layering of snow, user-adjustable layering of soil, snow cover compaction and destructive metamorphism, implicit solutions of soil heat and water transfer equations using the finite difference method, distinct parameterization of the surface organic layer, and a representation of unfrozen water in frozen soil. The model was tested using nine years (1994–2002) of field measurements obtained in a mature aspen forest ecosystem located in Prince Albert National Park, Saskatchewan, Canada. The variables tested include snow depth, snow cover duration, snow temperature, soil heat flux, and soil temperatures at different soil depths. The objectives of this study were (1) to study cold season snow and soil interactions and to improve the simulation of snow and soil thermal regimes in EALCO model and (2) to investigate the effects of different model configurations and parameterizations including snow and soil layering resolution, fractional snow cover parameterization, water table and total soil column depths, and the inclusion/exclusion of a surface organic layer and unfrozen water in frozen soil on the model results.

2. Model description

The EALCO model is developed at the Canada Centre for Remote Sensing to study the ecosystem-climate interactions for various terrestrial ecosystems. The main components of EALCO include the land surface radiation scheme, the snow and soil thermal and water scheme, the coupled canopy energy-water-CO_2 transfer scheme, and the plant and soil C and nitrogen (N) biogeochemical cycle scheme. A brief description of general model structure was given in Wang et al. (2004). Specifically, the EALCO land surface radiation scheme, which uses gap-probability based successive orders of scattering approach, was described in Wang (2005) and Wang et al. (2007). The coupling of canopy energy–water–CO_2 transfer dynamics in EALCO was documented in Wang (submitted for publication), which was improved from Wang et al. (2002a). The plant and soil C and N biogeochemical cycle scheme was detailed in Wang et al. (2001, 2002b), which was originally developed for the C coupled Canadian Land Surface Scheme (CLASS). This paper mainly introduces the simulation schemes for the snow cover dynamics and soil thermal and water regimes.

2.1. Determination of snow and soil layers and snow cover fraction

The total number of snow layers N_{sn} is determined in each time step according to the total snow cover depth H_{sn} (m) using:

$$\sum_{n=1}^{N_{sn}} h_{sn,n} \le H_{sn} < \sum_{n=1}^{N_{sn}+1} h_{sn,n} \tag{1}$$

where $h_{sn,n}$ is the depth for snow layer n, which is prescribed in the model. The snow cover fraction (f_{sn}) of the ground surface is calculated as

$$f_{sn} = \begin{cases} 1.0 & H_{sn} \ge h_{sn,th} \\ H_{sn}/h_{sn,th} & H_{sn} < h_{sn,th} \end{cases} \tag{2}$$

where $h_{sn,th}$ is defined as the threshold snow depth. It is required that $h_{sn,th}$ be greater than the top snow layer depth $h_{sn,1}$ to ensure that at least one snow layer is identified in the model. In the case of $f_{sn} < 1.0$, the model is run separately for the snow-free and snow-covered surfaces. The final model outputs (e.g. soil temperature and moisture) are the weighted average of these two fractions.

The depths of snow layers may change during a time step due to new snowfall, surface sublimation, snow melting, and snow density changes caused by compaction and destructive metamorphism. Therefore, the total number of snow layers is re-calculated at the beginning of each time step to maintain the prescribed snow layer depths. The snow state variables (e.g. snow temperature, snow and liquid water content, snow density, etc.) for each new layer are updated using the weighted average of the corresponding variables of the old snow layers that constitute the new snow layers. This dynamic snow-layering scheme allows the model to simulate the snow processes (e.g., heat transfer) in a consistent vertical resolution.

The total number of soil layers, the depth of each layer, and the entire soil column depth are prescribed before the model run. Theoretically, there is no upper limit for the number of soil layers and soil column depth in the model design. However, they should be specified according to the site conditions and the required computational efficiency. In this study, the lower boundary for soil

temperature simulation is set to the depth where the annual variation of soil temperature is negligible. The lower boundary for soil water simulation is set to water table depth. In case the water table falls below the lower boundary of temperature simulation, an additional layer is added for soil water simulation and its depth is determined by the lower boundary of temperature simulation and the water table. Where present, a distinct surface organic layer is parameterized in the model.

2.2. Surface energy balance

The energy balance equation for soil (snow) surface is solved numerically to obtain the soil (snow) surface temperature and the energy fluxes between soil (snow) and the atmosphere. The surface energy balance equation is expressed as

$$R_{\mathrm{ng}} - Q_h - Q_{le} - Q_g = 0 \tag{3}$$

where R_{ng} is the net radiation, Q_h and Q_{le} are sensible and latent heat fluxes, respectively, and Q_g is the conductive heat exchange at the interface between the atmosphere and the soil or snow. R_{ng} consists of net short wave radiation and net long wave radiation. The net short wave radiation plays a crucial role as it is the main energy input controlling the soil (snow) thermal regimes and variations. It is simulated by a gap probability based ray-tracing approach which improved the accuracy of canopy radiation transfer calculations as demonstrated in Wang (2005). The Q_{le} is calculated using the β method as described by Lee and Pielke (1992). The detailed formulations of net long wave radiation, Q_h and Q_g and the method for numerically solving the above equation are detailed in Verseghy (1991) and Wang et al. (2002a). The soil (snow) surface temperature and evaporation (sublimation) obtained from solving the above equation is used in the soil (snow) heat and water calculations as described below.

2.3. Heat transfer in soil and snow

Heat transfer in soil or snow due to temperature (T_i) gradient and the heat carried by the flowing water ($Q_{\mathrm{fl},i,}$W m$^{-2.}$) is simulated using:

$$C_i \frac{\partial T_i}{\partial t} = \frac{\partial}{\partial z}\left(k_{h,i}\frac{\partial T_i}{\partial z} + Q_{\mathrm{fl},i}\right) \tag{4}$$

where C_i and $k_{h,i}$ are the volumetric heat capacity (J m^{-3} K^{-1}) and thermal conductivity (W m^{-1} K^{-1}) of the soil (snow) layer i. C_i and $k_{h,i,}$ are parameterized using (Johansen, 1975; Mellor, 1977):

$$C_i = \sum_{j=1}^{5} C_{i,j}\theta_{i,j} \ \text{(for soil and snow)} \tag{5}$$

$$k_{h,i} = \prod_{j=1}^{5} \left(k_{h,i,j}\right)^{\theta_{i,j}} \ \text{(for soil)} \tag{6}$$

$$k_{h,i} = 0.074 + 2.576 \times 10^{-6}\rho_{\mathrm{sn},i}^2 \ \text{(for snow)} \tag{7}$$

where $C_{i,j}$and $k_{h,i,j}$ are the corresponding values of C_i and $k_{h,i}$ for soil mineral, soil organic matter (SOM) or litter, air, liquid water and ice (or snow), respectively, and $\theta_{i,j}$ is the volumetric fraction of each component. $Q_{\mathrm{fl},i}$ is calculated as:

$$Q_{\mathrm{fl},i} = C_w\left[W_{\mathrm{fl},i+1}(T_i - T_{i+1}) + W_{\mathrm{fl},i}(T_{i-1} - T_i)\right] \tag{8}$$

C_w is the volumetric heat capacity (J m^{-3} K^{-1}) of liquid water. $W_{\mathrm{fl},i}$ (m s^{-1}) is the water flux across the soil (snow) layers (discussed in Sections 2.4).

Eq.(4) is expressed discretely using finite difference method for each soil (snow) layer and solved implicitly using the method developed in the IBIS model (Foley et al., 2005). We assume that the surface water layer and the top soil layer have the same temperature and they are treated as one layer in solving the soil temperature equations. The upper boundary condition of Eq.(4) is the Q_g obtained in Eq.(3). The lower boundary condition is the assumed annual-constant soil temperature at the bottom of the simulated soil column. This temperature is prescribed in the first year of model run and updated for the each following year using the annual average temperature of the bottom soil layer in the previous year.

2.4. Water transfer in soil and snow

Water transfer in the soil is simulated by Richard's Equation:

$$\begin{cases} \dfrac{\partial \theta_{\mathrm{liq},i}}{\partial t} = \dfrac{\partial}{\partial z}\left[D\left(\theta_{\mathrm{liq},i}\right)\dfrac{\partial \theta_{\mathrm{liq},i}}{\partial z} - k\left(\theta_{\mathrm{liq},i}\right)\right] \\ D\left(\theta_{\mathrm{liq},i}\right) = k\left(\theta_{\mathrm{liq},i}\right)\dfrac{d\theta_{\mathrm{liq},i}}{d\psi\left(\theta_{\mathrm{liq},i}\right)} \end{cases} \tag{9}$$

where $k(\theta_{\mathrm{liq},i})$ and ψ $(\theta_{\mathrm{liq},i})$ are the unsaturated hydraulic conductivity and soil water potential of soil layer i. They

are parameterized according to Clapp and Hornberger (1978):

$$k(\theta_{\mathrm{liq},i}) = k_{0,i}(\theta_{\mathrm{liq},i}/\theta_{0,i})^{2b_i+3} \tag{10}$$

$$\psi(\theta_{\mathrm{liq},i}) = \psi_{0,i}(\theta_{\mathrm{liq},i}/\theta_{0,i})^{-b_i} \tag{11}$$

where $k_{0,i}$, $\theta_{\mathrm{liq},i}$, $\theta_{0,i}$ and $\psi_{0,i}$ are saturated hydraulic conductivity (m s^{-1}), volumetric liquid water content (m^3 m^{-3}), porosity (m^3 m^{-3}), and soil water potential (m) at saturation, respectively. The hydraulic conductivity $k(\theta_{\mathrm{liq},i})$ is set to 0 for frozen soil.

Eq.(9) is solved using the same method as for Eq.(4) discussed in Section 2.3. The upper boundary condition is the water infiltration rate which is simply estimated using the saturated hydraulic conductivity of top soil layer ($k_{0,1,}$) when a surface water layer is present. The lower boundary is the water table at which the water content is equal to porosity. Prior to solving Eq. (9), surface evaporation and plant root water uptake calculated for each soil layer during growing season (Wang et al., 2002a) are subtracted from the soil water content of each corresponding soil layer. After θ is determined, water flow between soil layers ($W_{\mathrm{fl},i}$, required in Eq. (8)) is calculated as:

$$W_{\mathrm{fl},i} = W_{\mathrm{fl},i+1} + h_i \Delta\theta_{\mathrm{liq},i}/\Delta t \tag{12}$$

where h_i is the depth of soil layer (i), Δt is the modelling time step, $\Delta\theta_{\mathrm{liq},i}$ is the change of liquid water content during Δt. Note that the above calculation is made upwards from the bottom soil layer, into which water flow from the water table ($n+1$) $W_{\mathrm{fl},n+1}$ is calculated by:

$$W_{\mathrm{fl},n+1} = k_n[1 + (\psi_0 - \psi_n)/(0.5h_n)] \tag{13}$$

At least 3 soil layers are required to implicitly solve Eq. (9). When the water table is in one of the top three layers, the model has less than three soil layers for water simulation. Under such circumstances, water flow between soil layers is firstly calculated using Eq. (13), from which the soil water content is then explicitly solved. This explicit method is also used to calculate the water flow between the surface organic layer and the mineral soil layer due to the limitation of Eq. (9) in the application to soils with distinct hydraulic property profiles (Celia et al., 1990; Talbot et al., 2004).

When rain falls on snow or snow melts, liquid water may temporally exist in snow layers. The movement of liquid water between snow layers ($W_{\mathrm{fl},i}$) is simulated simply by introducing a snow water holding capacity $W_{c,i}$ (m^3 m^{-3}), which is determined by (Kongoli and Bland, 2000):

$$W_{c,i} = \begin{cases} W_{c,\min} + (W_{c,\max} - W_{c,\min})(\rho_c - \rho_{\mathrm{sn},i})/\rho_c & \rho_{\mathrm{sn},i} < \rho_c \\ W_{c,\min} & \rho_{\mathrm{sn},i} \geq \rho_c \end{cases} \tag{14}$$

where $W_{c,\min}$ (0.04 m^3 m^{-3}) and $W_{c,\max}$ (0.1 m^3 m^{-3}) are minimum and maximum values of snow water holding capacity, ρ_c is a threshold value of snow density (200 kg m^{-3}). If the liquid water content in a snow layer exceeds $W_{c,i}$, the excessive water will percolate to the layer below by gravity. The liquid water flow out of the bottom snow layer is added to the surface water layer for soil infiltration and runoff calculations.

2.5. Thaw freeze of soil water and snow

The thaw and freeze processes in each of the soil and snow layers are simulated after T_i and $\theta_{liq,i}$ in Eqs. (4) and (9) are solved. T_i and $\theta_{\mathrm{liq},i}$ are used to check for the thaw and freeze conditions and to calculate the thawing and freezing portions. The volumetric portion of liquid water ($\theta_{u,i}$) existing in frozen soil is determined by (Ling and Zhang, 2004).

$$\theta_{u,i} = c(T_0 - T_i)^d \qquad T_i \leq T_0 \tag{15}$$

where c, d are soil texture related parameters, and T_0 is the melting point (0°C used in the model).

When $T_i < T_0$ and $\theta_{\mathrm{liq},i} > \theta_{u,i,}$, the portion of water to be frozen is calculated as:

$$\theta_{\mathrm{fz}} = \min(\theta_{\mathrm{liq},i} - \theta_{u,i}, \quad (T_0 - T_i)C_i/(\rho_w L_{\mathrm{fus}})) \tag{16}$$

When $T_i > T_0$ and $\theta_{\mathrm{ice},i} > 0$, the portion of ice to be thawed is calculated as:

$$\theta_{tw} = \min(\theta_{ice,i}, \quad (T_i - T_{0t})C_i/(\rho_w L_{fus})) \tag{17}$$

where ρ_w and L_{fus} are density (kg m^{-3}) and fusion heat (J kg^{-1}) of water. $\theta_{u,i}$is set to 0 for snow layers. If $\theta_{\mathrm{ice},i}$and $\theta_{\mathrm{liq},i}$coexist after the above calculations of thaw and freeze, T_i is set to T_0. Otherwise, T_i is reset to

$$T_i' = \begin{cases} T_i + \theta_{\mathrm{fz}}\rho_w L_{\mathrm{fus}}/C_i' & \text{(thaw)} \\ T_i - \theta_{\mathrm{tw}}\rho_w L_{\mathrm{fus}}/C_i' & \text{(freeze)} \end{cases} \tag{18}$$

where T_i' and C_i' are updated temperature and heat capacity of the soil (snow) layer after freezing or thawing.

2.6. Snow density change

The snow density change due to compaction metamorphism of snowpack is calculated after Mellor (1977) and Kongoli and Bland (2000):

$$\partial\rho_{\mathrm{sn},i}/\partial t = c_1\rho_{\mathrm{sn},i}W_s e^{\left[0.08\left(T_{\mathrm{sn},i}-T_0\right)-0.021\rho_{\mathrm{sn},i}\right]} \tag{19}$$

where $\rho_{\mathrm{sn},i}$(kg m^{-3}) and $T_{\mathrm{sn},i}$ are the density and temperature of snow layer i, and W_s (mm) is the snow amount (water equivalent) above layer i. The empirical coefficient c_1 (0.001 mm^{-1}hr^{-1}) is converted from the value used by Kongoli and Bland (2000).

The snow density change due to destructive metamorphism is calculated after Anderson (1976):

$$\partial\rho_{\mathrm{sn},i}/\partial t = \begin{cases} c_2\rho_{\mathrm{sn},i}e^{\left[0.04\left(T_{\mathrm{sn},i}-T_0\right)-0.046\left(\rho_{\mathrm{sn},i}-\rho_d\right)\right]} & \rho_{\mathrm{sn},i}>\rho_d \\ c_2\rho_{\mathrm{sn},i}e^{\left[0.04\left(T_{\mathrm{sn},i}-T_0\right)\right]} & \rho_{\mathrm{sn},i}\leq\rho_d \end{cases} \tag{20}$$

The empirical coefficient c_2 (0.001 h^{-1}) and threshold snow density ρ_{d} (150 kg m^{-3}) are taken from Kongoli and Bland (2000). The snow density change due to liquid water freezing is simply represented by adding the increased ice to the snow without increasing the snow volume (depth).

3. Site, data and model configuration and parameterization

The model was tested using observations made in a boreal deciduous forest ecosystem (53.6°N, 106.2°W), which is located at Prince Albert National Park, Saskatchewan, Canada. The vegetation is mainly trembling aspen (*Populus tremuloides* Michx.) with scattered balsam poplar (*Populus balsamifera* L.) in the overstory and hazelnut (*Corylus cornuta* Marsh) in the understory. The forest regenerated after a natural fire in 1919 and had a stand density of ~830 stems ha^{-1} in 1994. The soil is an Orthic Gray Luvisol with an 8–10 cm thick surface organic layer overlying a loam to sandy clay loam mineral soil. The terrain is generally level. Mean annual air temperature and precipitation (1942–1990 climatic normals) at the nearest long-term weather station (Prince Albert Airport, 53.2°N and 105.7°W) are 0.5 °C and 406 mm, respectively.

A nine-year long (1994–2002) half-hourly meteorological dataset including incoming shortwave and longwave radiation, precipitation, air temperature, wind speed, atmospheric pressure and specific humidity was constructed as a model input. It is based mainly on two datasets: (1) Boreal Ecosystem-Atmosphere Study (BOREAS) AFM-7 SRC surface meteorological and radiation data (1994–1996, Shewchuk, 2000) and (2) Fluxnet-Canada Research Network Data Information System (FCRN-DIS) meteorological data (1997–2002, http://fluxnet.ccrp.ec.gc.ca/). Missing data were filled using the measurements at Prince Albert Airport weather station (http:// www.climate.weatheroffice.ec.gc.ca/climateData/canada_e.html). Daily snow depth, soil temperatures at depths of 0.05 m, 0.1 m, 0.2 m, 0.5 m and 1.0 m were also compiled from the above data sources. Snow depths and soil temperatures at 0.1 m, 0.2 m and 0.5 m were available from 1994 to 2002. The 0.05 m and 1.0 m soil temperature measurements were only available for the period of 1997–2002. The 0.05 m soil temperature probe was located in the surface organic layer, while other soil temperature probes were inside the mineral soil. Snow temperature measurements were available from November 2001 at various heights above the ground surface. The soil heat fluxes at soil surface were available from January 1997. More detailed information about the site, known as Southern Old Aspen (SOA), and the measurements can be found in Black et al. (1996), Shewchuk (1997), Griffis et al. (2003) and Barr et al. (2004).

Table 1
Observed snow variables, minimum daily air and soil temperatures during the 8 snow seasons (October 1- May 31)

Season	Snowfall amount[a] (mm)	Snow-cover duration[b] (days)	Maximum snow depth (m)	Minimum T_a (°C)	Minimum T_s at 0.1 m (°C)	Minimum T_s at 0.5 m (°C)	Minimum T_s at 1.0 m (°C)
1994–1995	139.3	182	0.576	−27.0	−0.8	−0.1	–
1995–1996	184.0	–	0.648	−32.1	−2.0	−0.8	–
1996–1997	88.4	–	0.587	−31.5	−2.2	−0.6	0.3
1997–1998	78.0	–	0.298	−26.9	−2.4	−0.8	0.3
1998–1999	163.1	192	0.467	−27.7	−1.1	0.1	0.7
1999–2000	91.1	169	0.474	−25.4	−1.3	0.2	1.0
2000–2001	65.0	168	0.365	−30.3	−1.7	−0.2	0.7
2001–2002	71.1	178	0.356	−29.4	−4.0	−1.8	−0.6
Average	109.0	(177.8)	0.471	−28.8	−1.9	−0.5	(0.4)

[a]Calculated from precipitation observation when air temperature was less than 0 °C.
[b]Estimated from the snow depth observations. –: could not be estimated due to missing observations at starting and/or ending periods of snow cover.

The precipitation is treated as rain (snow) when the air temperature is higher (lower) than 0°C in the model. Large inter-annual variations in snowfall amount, snow cover duration, snow depth, air and soil temperatures were observed during the study period (1994–2002). Table 1 summarizes the key snow/soil variables during each snow season (defined as October 1–May 31 in this study). The snowfall amount varied from 65 mm (2000–2001) to 184 mm (1995–1996). Snow cover duration varied from 168 days (2000–2001) to 192 days (1998–1999). The maximum snow depth varied from 0.298 m (1997–1998) to 0.648 m (1995–1996). The minimum daily air temperature varied from −25.4 °C (1999–2000) to −32.1 °C (1995–1996), while the minimum soil temperatures varied from −0.8 °C (1994–1995) to −4.0 °C (2001–2002) at 0.1-m soil depth and 0.2 °C (1999–2000) to −1.8 °C (2001–2002) at 0.5-m soil depth. Frozen soil (below 0 °C) was observed at 0.5-m depth in most winters except 1998–1999 and 1999–2000. The soil remained unfrozen at the 1.0-m depth in all winters except 2001–2002 when relative thinner snow cover was observed.

Table 2 lists the key model configurations and parameters used in the model test. The top soil layer was parameterized as fabric peat (Letts et al., 2000). Other layers were set as loamy clay with sand, clay, silt and SOM content of 48.4%, 21.1%, 30.2% and 0.3%, respectively, which were averaged from in situ soil profile observations by Anderson and Nerbas (2000). Water table depth was kept constant at 4m, which was estimated from Barr et al. (2000). The daily leaf-area index for each year of 1994–2002 was estimated from Barr et al. (2004).

Table 2
Model configurations and parameters used in the test run

Item	Setting
$h_{sn,\ 1}$ in Eq. (1)	0.05 m
$h_{sn,n}$ in Eq. (1) ($n>1$)	0.1 m
$h_{sn,th}$ in Eq. (2)	0.2 m
Number of soil layers	16
Depth of soil column simulated	4.15 m
Depth of organic layer	0.1 m
Depth of mineral layers	0.05, 0.1, 0.1, 0.1, 0.1,0.1, 0.1, 0.1, 0.1, 0.1, 0.1, 0.2, 0.4, 0.8, 1.6 m
$K_{0,1}$, $\psi_{0,1}$, $\theta_{0,1}$ and b_0 for organic layer (Eqs. (11) and (12))	2.8×10^{-4} m s^{-1}, 0.0103 m,0.93 and 2.7 (Letts et al., 2000)
$K_{0,i}$, $\psi_{0,i}$, $\theta_{0,i}$ and b_i for mineral layers (Eqs. (11) and (12))	5.1×10^{-6} m s^{-1}, 0.17 m, 0.43 and 2.7
C, d and T_0 for organic layer (Eq. (15)	2.6, −0.38 and 0 °C (Ling and Zhang, 2004)
C, d and T_0 for mineral layer (Eq. (15)	6.4, −0.38 and 0 °C (Ling and Zhang, 2004)
Water table depth	4.0 m (constant)

Table 3
Regression statistics of simulated (Y) vs. observed (X) soil heat flux (Q_{gs}, W m^{-2}), snow depth (H_{sn}, m), snow temperature (T_{sn}, °C) and soil temperatures (T_s, °C) at 5 depths during 1994–2002

Item	a	b	R^2	σ	N
Q_{gs}	0.63	−0.13	0.70	2.49	2116
H_{sn}	0.82	2.64	0.71	0.085	1407
T_{sn}	0.99	−0.05	0.92	1.3	223
T_s at 0.05 m	1.21	−0.77	0.94	1.7	2187
T_s at 0.1 m	1.0	−0.21	0.96	1.1	3170
T_s at 0.2 m	1.01	−0.10	0.96	1.0	3169
T_s at 0.5 m	0.95	0.42	0.97	0.8	3170
T_s at 1.0 m	0.90	0.55	0.98	0.4	2164

Note: regression equation: $Y=aX+b$; R^2: coefficients of determination; σ: standard deviation, same units as items; N: number of valid observations.

4. Model test results

Table 3 compares model outputs with observations during the 9-year study period. Two snow seasons (1998–1999 and 2001–2002) with contrasting snowfall amount (Fig. 1) were selected to evaluate the detailed model performance and the impact of snow cover on soil temperature.

4.1. Surface energy balance

Fig. 2 shows the energy fluxes of the snow/soil surfaces during the two selected seasons. Simulated net radiation above the forest canopy (R_{nc}) is also shown and compared with observations (Fig. 2a and b). Good agreement between simulated and observed R_{nc} indicates that the radiative energy exchange of the ecosystem was accurately simulated (Fig. 2a and b). The simulated net radiation at the snow/soil surface (R_{ng}) shows that both the radiative energy loss (negative values) and gain (positive values) were largely reduced from R_{nc} by the canopy. For example, from December 1st to January 15th, the net radiative energy loss from the snow surface under the canopy was only 45–50% of that over canopy.

The seasonal variation of snow and soil surface energy fluxes were largely influenced by the variation of net radiative energy exchange R_{ng}. During the mid-winter (December–February), the snow surface lost net radiation (Fig. 2a and b) and had very small sensible (Q_h) and latent (Q_{le}) heat exchange (Fig. 2c and d). The negative R_{ng} was mainly balanced by the upward conductive heat flux to the snow surface (Fig. 2e and f), which in turn caused the energy losses from the soil below (Fig. 2g and h). Later in spring, with the increase in incoming

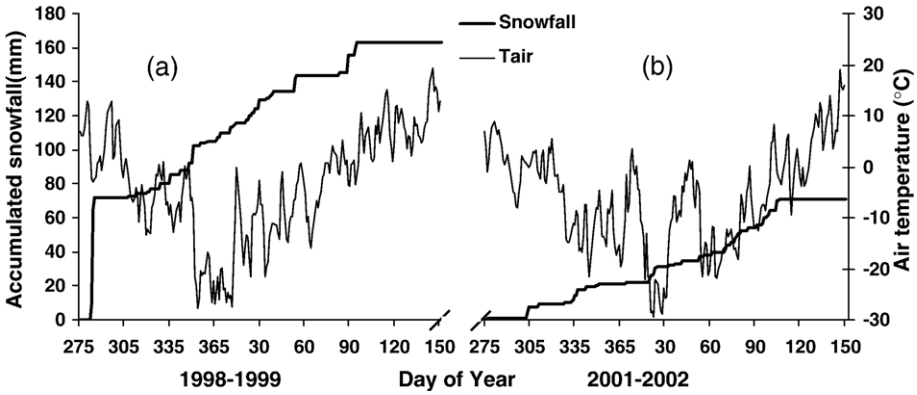

Fig. 1. Observed accumulated snowfall amount and daily air temperature during the two model test seasons of 1998–1999 (a) and 2001–2002 (b) at the Southern Old Aspen (SOA) forest site.

radiative energy, both R_{nc} and R_{ng} became positive (Fig. 2a and b). The changing of net radiation from negative to positive at the snow surface was slightly later than that at the canopy surface due to canopy interception of radiation and heat storage of the forest canopy. The energy gained at the snow surface (Fig. 2e and f) raised the surface snow temperature to the melting point and caused snow to melt (Fig. 3). During the snow melting periods (e.g. DOY 60-113 in Fig. 3a and DOY 90-133 in Fig. 3b), latent heat Q_{le} increased due to the presence of liquid water in the top snow layer. The sensible heat Q_h was mostly negative or had smaller positive values than the Q_{le} (Fig. 2c and d). The heat exchange at the soil surface was very small during snow melting periods since both snow and soil temperatures were close to the melting point (0 °C). After the snow melted, Q_{le} decreased due to drying of the surface soil, Q_h became the dominant component of net radiation dissipation and the soil surface started to gain energy with the resulting increase in soil temperature. The simulated variations of soil surface heat fluxes during the two seasons tracked the observations well (Fig. 2g and h). Regression of simulated and observed daily soil surface heat fluxes during the entire 9 years showed a coefficient of determination (R^2) of 0.70 and a standard deviation (σ) of 2.49 W m^{-2} (Table 3). Energy inputs through rain on snow ($Q_{fl,1}$) can be significant for snow melt in some cases (Sui and Koehler, 2001). However, we found it was not significant at this site (Fig. 2e and f).

Snow cover had a great impact on the soil heat flux. During the mid-winter months (December, January and February), the energy loss from the soil surface was much larger in 2001–2002 than in 1998–1999, which was mainly due to the much shallower snow cover in the 2001–2002 season. The model successfully captured the observed responses of energy fluxes to snow cover depth (Table 4).

4.2. Snow cover and snow temperature

Table 1 lists snow cover duration during the 5 snow seasons estimated from snow depth observations. The comparison between simulated and observed snow cover duration was influenced by the definition of snow cover. If we use a threshold of 50% snow cover fraction to delineate snow versus no snow, the simulation underestimated the snow cover duration by 5–15days. Using a threshold of 5% snow cover fraction, the simulation overestimated the snow cover duration by 1–13 days. In this study, a threshold of 25% snow cover fraction produced the best agreement between simulated and observed snow cover duration, within ±5 days.

A comparison between observed and simulated snow depths for the two seasons is shown in Fig. 3. During the 1998–1999 season, observed snow cover started in early October and ended in mid-April with a significant melting period occurring in late October (Fig. 3a). During the 2001–2002 season, the observed snow cover started in early November and ended in early May (Fig. 3b). In general, simulated snow cover evolution patterns (e.g. starting, ending, accumulation, and melting) and the snow depth agreed well with observations in both seasons. Regression of simulated vs. observed snow depths during the entire 9 years showed an R^2 of 0.71 and a standard deviation σ of 0.085 m (Table 3).

Several factors contributed to the discrepancies between the simulated and observed snow depths. Firstly, error in snow depth simulation at one time step produce systematic errors for the snow depth simulation afterwards. For example, the overestimation of snow depth in DOY 285, 1998 caused overestimation of snow depth until DOY 51, 1999 (Fig. 3a). Secondly, the partitioning of precipitation between rain and snow using a 0 °C air temperature threshold has been challenged by

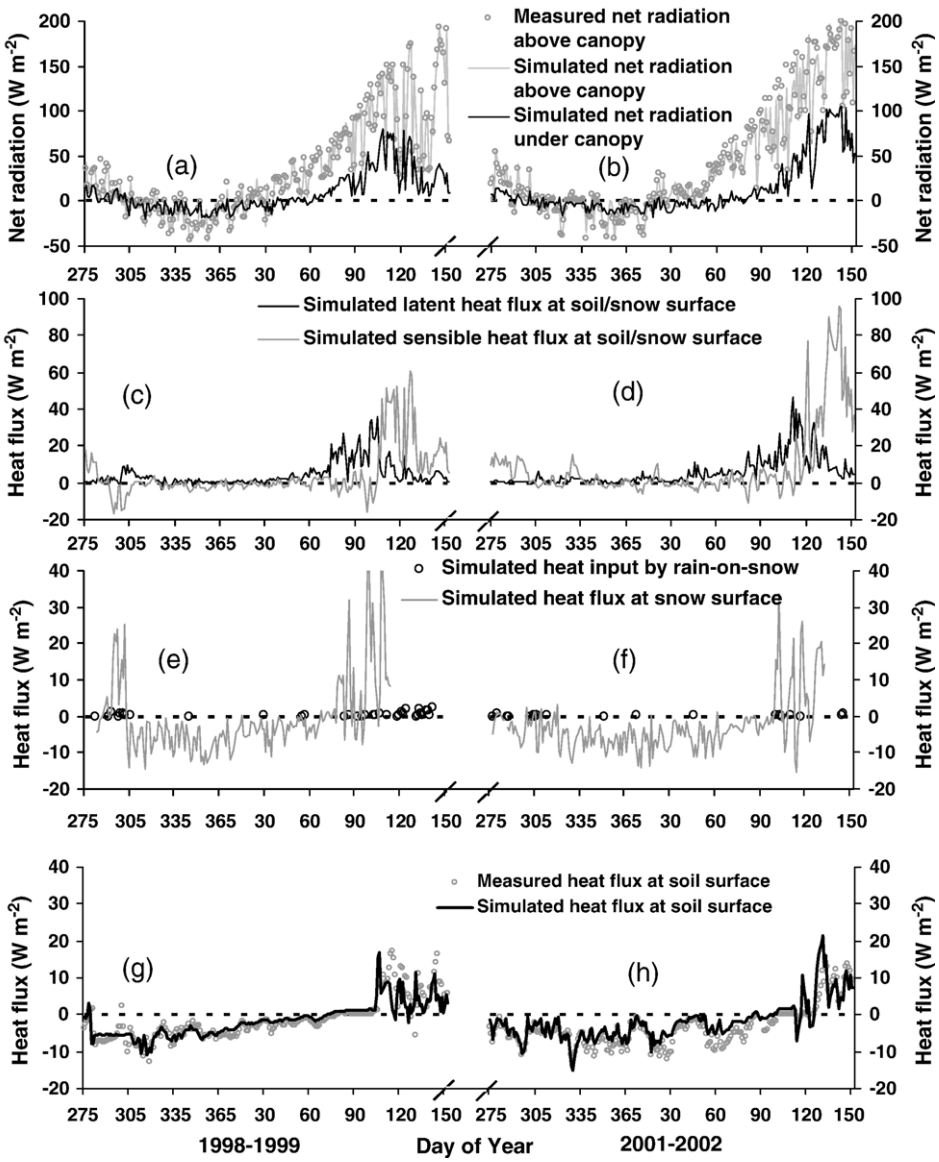

Fig. 2. Daily-averaged energy fluxes during the two model test seasons of 1998–1999 (a, c, e and g) and 2001–2002 (b, d, f and h) at the Southern Old Aspen (SOA) forest site.

observational and modeling studies (Auer, 1974; Kongoli and Bland, 2000; Yang and Niu, 2003; Bartlett et al., 2006). By analyzing 10 years precipitation data in 39 meteorological stations across Canada, Bartlett et al. (2006) concluded that a polynomial distribution method for rain/snow partitioning in the air temperature range of 0 ~ 6 °C (Auer, 1974) generally gave a better classification than the 0 °C threshold employed in this study. However, both the test from Bartlett et al. (2006) and the test from this study at the same SOA site showed very little difference (<0.01 m) in snow depth simulation between the two methods. Due to the fast transition of air temperature during the snow accumulation periods at this site, the Auer's polynomial only gave about 10% more snowfall during the entire snow season and more than half of those happened during the snow-melting period, which melted immediately and had very little effects on the snow depth simulation. Thirdly, observational uncertainties in winter precipitation and snow depths could also cause the discrepancies between the simulated and observed snow depths.

Simulated snow temperatures were evaluated using observations from the 2001–2002 snow season. Since the observed snow temperatures were measured at fixed

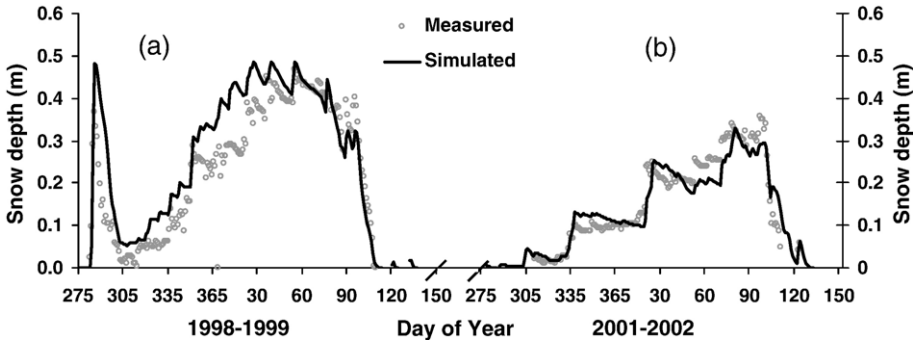

Fig. 3. Observed and simulated snow depths during the two model test seasons of 1998–1999 (a) and 2001–2002 (b) at the Southern Old Aspen (SOA) site.

heights above the soil surface, while the simulated snow layer temperatures represent the varying depths determined by the dynamic snow layering calculation, direct comparisons of snow temperature for each layer was not possible. Therefore a weighted-averaged snow temperature for all layers over the entire snowpack was compared between the simulated values and the observations (Fig. 4). The simulated snow temperature variations showed good agreement with observations. Regression of simulation *vs*. all the available observations of snow temperature showed a R^2 of 0.92 and a standard deviation of 1.3 °C (Table 3).

4.3. Soil temperatures

Fig. 5 compares the simulated and observed soil temperatures at four soil depths during the two seasons. In general, simulated soil temperature showed good agreement with the observations at all depths. The agreement was better in the mineral soil layers than in the organic layer, and better in the deeper layers than in the shallow layers. Regression of simulated vs. observed soil temperatures for all the available test data at 5 depths showed that R^2 ranged from 0.94 to 0.98 and σ ranged from 0.4 to 1.7 °C (Table 3). Snow cover had a large impact on surface energy fluxes and soil temperature. It reduced energy losses from the soil surface and kept soil temperatures much higher than air temperatures in winter. During the eight snow seasons used in model testing, both observed and simulated minimum daily soil temperatures did not fall below −5.0 °C at 0.1 m and −2 °C at 0.5 m soil depth (Table 3 and Fig. 5), although the minimum daily air temperatures reached −25 °C. The model successfully captured the impacts of snow cover depth on soil temperature and soil freezing depth (Table 4). Although the average air temperature during the mid-winter months of 1998–1999 was about 0.9°C lower than that of 2001–2002, the observed average soil temperatures at the four soil depths during the same period of 1998–1999 were 0.6–1.7 °C (simulated 0.7–3.0 °C) higher than that of 1998–1999, mainly attributed to the doubled snow depth in the 1998–1999 season. As a result, the maximum soil freezing depth reached 1.0 m (simulated 0.9 m) in the 2001–2002 season while it reached only about 0.4 m (simulated 0.3 m) in the 1998–1999 season.

The larger errors in simulating the temperature of the organic layer were caused by the difficulties in parameterizing the organic soil. Letts et al. (2000) reported that the hydraulic and thermal properties of organic soil could be significantly different depending on the composition of the organic material. Because the physical properties of the surface organic layer vary widely among forests sites, their accurate parameterization is difficult. The smaller discrepancy between simulated and observed soil temperature in the deeper layers was partially due to the decreased soil temperature variations with depth.

Table 4
Comparison of observed and simulated snow/soil variables during mid-winter months (December, January and February) of the two snow seasons

Variables	1998–1999		2001–2002	
	Observed	Simulated	Observed	Simulated
$T_{a,\mathrm{av}}$ (°C)	−13.2	–	−12.3	–
$H_{\mathrm{sn,av}}$ (m)	0.30	0.35	0.15	0.16
$R_{\mathrm{nc,av}}$ (W m^{-2})	−1.5	−2.3	−1.4	−1.3
$Q_{s,\mathrm{av}}$(W m^{-2})	−3.7	−3.1	−6.2	−6.3
$T_{s,\mathrm{av}}$ at 0.05 m (°C)	−0.6	−0.7	−2.3	−3.7
$T_{s,\mathrm{av}}$ at 0.1 m (°C)	−0.4	−0.3	−2.0	−2.0
$T_{s,\mathrm{av}}$ at 0.5 m (°C)	0.6	0.9	−0.3	0.1
$T_{s,\mathrm{av}}$ at 1.0 m (°C)	1.7	2.1	1.1	1.4
$H_{\mathrm{fz,\ max}}$ (m)	0.39	0.32	1.0	0.89

Note: $T_{a,\mathrm{av}}$, average air temperature; $H_{\mathrm{sn,av}}$, average snow depth; $R_{\mathrm{nc,av}}$, average net radiation above canopy; $Q_{s,\mathrm{av}}$, average conductive heat flux at soil/snow interface; $T_{s,\mathrm{av}}$, average soil temperatures; $H_{\mathrm{fz,max}}$, maximum freezing depth.

5. Effects of model configuration and parameterization on snow cover and soil temperature simulations

The influences of the model configuration and parameterization on the snow cover and soil temperature simulations were investigated by using the configurations and parameters listed in Table 5. The 1999–2000 snow season which had a near normal snowfall amount was selected to make the comparison.

The depth of snow layers ($h_{sn,n}$ in Eq. (1)) and the threshold snow depth ($h_{sn,th}$ in Eq. (2)) are key parameters that control the dynamic snow layering. By increasing $h_{sn,n}$ ($n>1$) from 0.1 m (baseline run, Table 2) to 0.2 m, the maximum number of snow layers simulated during the 1999–2000 snow season was reduced from 5 to 3. The coarser resolution of snow layering delayed the snow-melting processes, causing a 13-day increase in snow cover duration. The delay of snowmelt was mainly due to the larger heat capacity of a thicker snow layer, which delayed the response of snow temperature on surface heating. By changing $h_{sn,th}$ from 0.2 m (baseline run) to 0.05 m, the snow cover fraction (f_{sn}, Eq. (2)) during shallow snow cover periods was greatly increased, which caused a 9-day decrease of the snow cover duration. The faster snow melt with the smaller $h_{sn,th}$ is partially due to the increased f_{sn}, which results in more radiative energy for snow melting, due in part to the thinner snow layer during partial snow cover, which responds faster to surface heating. The changes in $h_{sn,n}$ and $h_{sn,th}$ caused very little change in both the average and maximum snow depths, indicating that the two parameters have little effect on snow simulation during the no-melt period. The simulated seasonal average and minimum soil temperatures were also affected little by the changes of $h_{sn,n}$ and $h_{sn,th}$.

Similar to snow cover, the surface organic layer also serves as a thermal buffer for the mineral soil below. By replacing the baseline parameters for the surface organic layer with the parameters for the mineral soil, the simulated soil temperatures in all soil layers were significantly lower than for the baseline run. However, a reduction of the surface organic layer thickness from 0.1 m (baseline run) to 0.05 m caused very little change in the soil temperature simulations. The results indicate that the inclusion of a surface organic layer is necessary, although the sensitivity of the simulated soil temperature in winter is greatly reduced after the organic layer thickness exceeds certain threshold (e.g. 0.05 m for this site).

The depth of the water table affects soil temperature simulation mainly by altering thermal properties through the soil water content of the soil (Eqs. (5) and(6)). By decreasing the water table depth from 4 m (baseline run) to 3 m, the simulated seasonal-average soil temperatures at 0.1 m ($T_{0.1,av}$), 0.5 m ($T_{0.5,av}$) and 1 m ($T_{1,av}$) were lowered by 0.1 °C, 0.2 °C and 0.3 °C respectively. However when the water table was set to 5 m, there were no significant changes in simulated soil temperatures, particularly in the upper soil layers. The results showed that the water table effect was only obvious when it was shallow enough to cause substantial water content changes in the simulated soil layers. The results also imply that dynamic water table inputs are likely to be critical for the soil temperature simulations in some ecosystems where the water table is high and variable.

The assumption that the annual variation in soil temperature is negligible at the bottom of the soil column is critical for solving Eq. (4). This assumption is only appropriate when the simulated soil column is sufficiently deep. Decreasing the soil column depth from 4.15 m (baseline run) to 3.15 m caused the discrepancies between

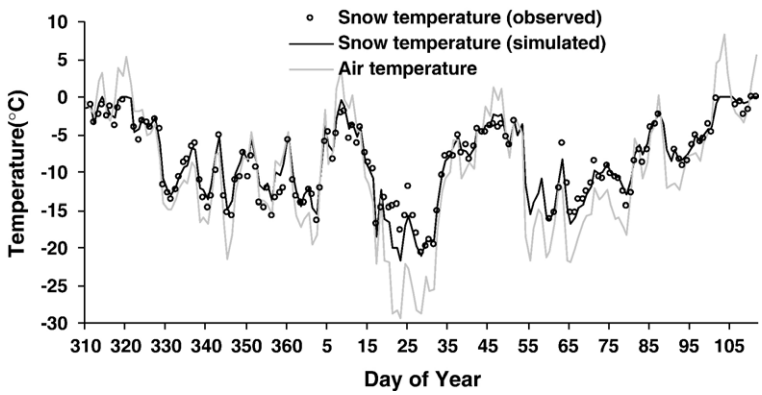

Fig. 4. Observed and simulated average snow temperature during the snow cover period of 2001–2002 at the Southern Old Aspen (SOA) site. The air temperature during this period was also plotted. The snow temperatures were the weighted average values for all the observed and simulated snow layers.

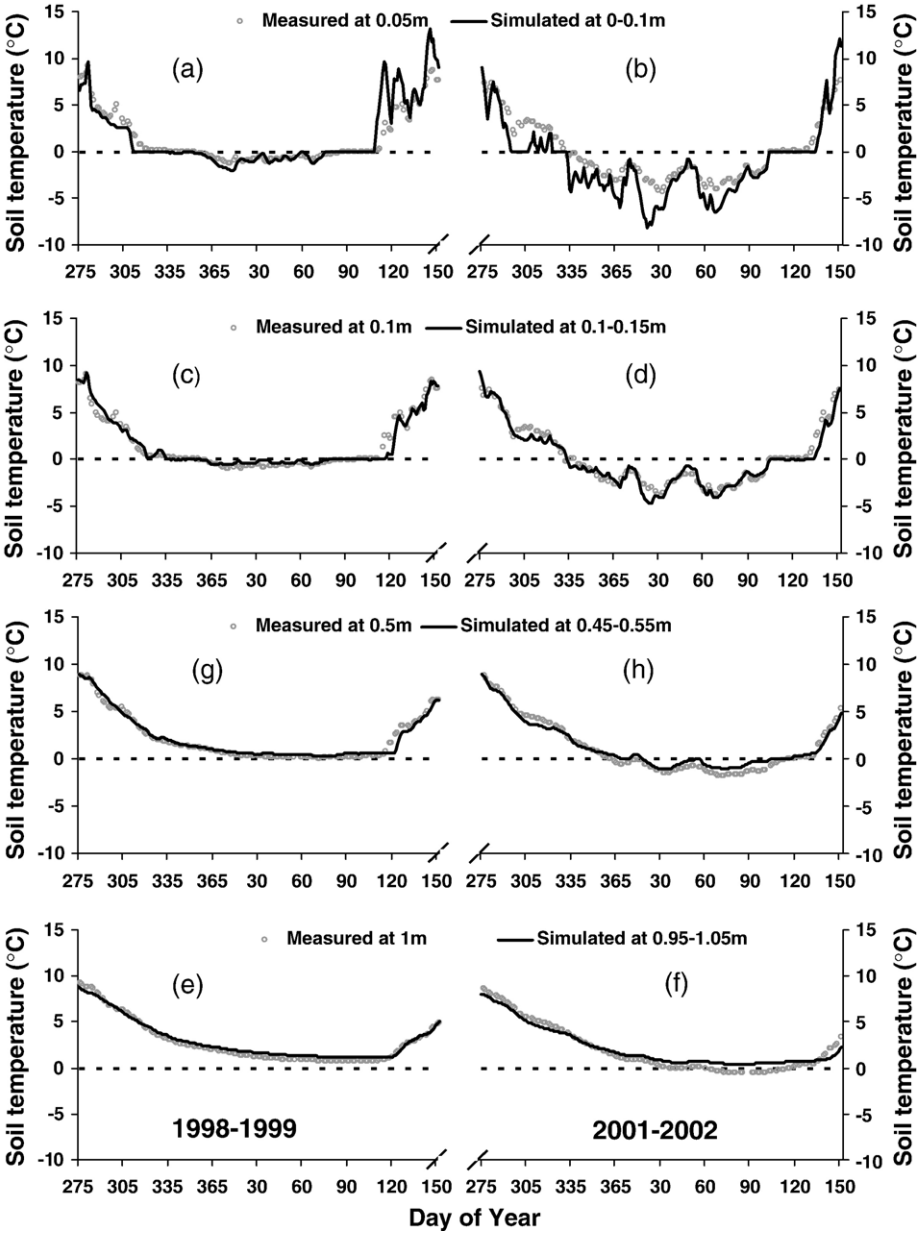

Fig. 5. Simulated and observed soil temperatures at 4 soil depths during the two model test seasons of 1998–1999 (a, c, e and g) and 2001–2002 (b, d, f and h) at the Southern Old Aspen (SOA) site.

the simulated and observed soil temperatures to increase considerably. However, increasing the soil depth to 5.15 m had little impact on the simulated soil temperatures. The results were sensitive to soil column depth but only up to a threshold value. For this study site, 4.15 m was an appropriate soil column depth to simulate the soil temperatures above 1 m.

Several studies have demonstrated the importance of including unfrozen water in frozen soils (e.g., Li and Koike, 2003; Ling and Zhang, 2004). However, our model experiments show that the exclusion of an unfrozen water parameterization in frozen soil (Eq. (15)) did not significantly change the soil temperature results. This is probably due to the fact that the soil was frozen much shallower and for shorter periods at this boreal forest site than in the permafrost regions of the above-mentioned studies.

The impact of soil layering resolution on the soil temperature simulation was investigated by additional model

Table 5
Effects of model configuration and parameterization on snow and soil temperature simulations

Observation/setting	D_{sn} (days)[a]	$H_{sn,av}/H_{sn,max}$ (m)[a]	$T_{0.1,av}/T_{0.1,min}$ (°C)[a]	$T_{0.5,av}/T_{0.5,min}$ (°C)[a]	$T_{1,av}/T_{1,min}$ (°C)[a]
Baseline run[b]	170	0.208/0.529	2.0/−0.4	2.6/0.6	3.2/1.4
$h_{sn,n}$=0.2 m (n> 1) (Eq. (1))	183	0.219/0.514	1.8/−0.4	2.5/0.6	3.2/1.5
$h_{sn,th}$=0.05 m (Eq. (2))	163	0.189/0.50	1.9/−0.5	2.5/0.6	3.2/1.4
Depth of organic layer=0.05 m	170	0.206/0.524	1.9/−0.6	2.6/0.6	3.3/1.4
Depth of organic layer=0 m	171	0.205/0.522	1.2/−3.8	1.9/0.0	2.8/1.1
Water table depth=3 m	170	0.208/0.528	1.9/−0.4	2.4/0.5	2.9/1.3
Water table depth=5 m	170	0.208/0.529	2.0/−0.5	2.6/0.6	3.3/1.5
Soil depth=3.15 m	171	0.209/0.53	1.4/−0.7	1.7/0.2	2.1/0.7
Soil depth=5.15 m	170	0.208/0.529	2.1/−0.4	2.7/0.8	3.4/1.7
$\theta_{u,i}$=0 (Eq. (15))	170	0.208/0.528	2.0/−0.4	2.6/0.7	3.3/1.5
Total soil layers=3	170	0.204/0.521	–[c]	–[c]	–[c]
Total soil layers=6	170	0.206/0.524	2.1/−0.2	–[c]	–[c]
Observation	169	0.221/0.474	1.9/−1.3	2.5/0.2	3.2/1.0

[a] D_{sn}, $H_{sn,av}$, $T_{0.1,av}$, $T_{0.5,av}$, $T_{1,av}$ represent snow cover duration, averaged snow depth, averaged soil temperature at 0.1 m, 0.5 m and 1 m soil depths over the period of Oct. 1, 1999–May 31, 2000; $H_{sn,max}$, $T_{0.1,min}$, $T_{0.5,min}$, $T_{1,min}$ represent their maximum (max) or minimum (min) values over the same period.
[b] The configurations and parameterizations of baseline run were the same as in Table 2.
[c] –: the soil layer depth did not match the baseline run.

runs using 3 and 6 soil layers. In order to keep the same soil column depth and organic layer depth as in the baseline run (16 soil layers), the depths of 3 soil layers were set to 0.10 m, 0.30 m and 3.75 m, and the depths of 6 soil layers were set to 0.10 m, 0.05 m, 0.20 m, 0.3 m, 0.7 m and 2.8 m. The top layer was set to an organic layer as in the baseline run. The soil temperatures of each of the 16 soil layers in the baseline run were weight-averaged with layer thickness into temperatures corresponding to those of the layers in the 3-layer and 6-layer runs. Fig. 6a shows that large discrepancies in the temperature simulations were found between the 3-layer run and the baseline run. The root mean squared differences (RMSDs) between the 3-layer run and the baseline run were 0.9 °C, 1.2 °C and 1.0 °C, respectively, from the top to the bottom. The 6-layer run brought the soil temperature simulation much closer to the baseline run results, especially in the upper soil layers (Fig. 6b). RMSDs between the 6-layer run and the baseline run for the 6 soil layers were 0.4 °C, 0.5 °C, 0.5 °C, 0.5 °C, 0.7 °C and 0.8 °C, respectively, from top to bottom. This result indicates that a 6-soil-layer resolution could achieve the simulation accuracy of 0.5 °C in the upper 0.65 m soil. When deeper soil temperature is considered (e.g. permafrost dynamics), more detailed soil layering is required.

6. Conclusions

This study presents new soil and snow schemes in the ecosystem model EALCO that includes dynamic layering of snow, user-adjustable layering of soil, snow cover compaction and destructive metamorphism, implicit solution of soil heat and water transfer equations using a finite difference method, distinct parameterizations of surface organic layer and the unfrozen water content in frozen soil. The model was tested with 9 years of observations at a boreal deciduous forest ecosystem and the effects of different model parameterizations and configurations were also investigated. The results showed that:

(1) The model accurately reproduced the observed snow and soil thermal regimes during the 9-year model testing period. The coefficients of determination (R^2) for the relationships between the simulations and observations of soil heat flux, snow depth, snow temperature, and soil temperatures at 5 depths were 0.70, 0.71, 0.92 and 0.94–0.98 respectively. The soil temperatures were better simulated in the mineral soil horizons than in the surface organic layer, and better simulated in the deeper mineral layers than in the shallower mineral layers.
(2) Snow cover had large effects on the surface energy fluxes, soil temperature and soil frozen depth. Both the observations and simulations demonstrated a much higher soil temperature than air temperature during the winter months of all the tested years. Deeper snow cover (e.g. 1998–1999 winter) resulted in less heat loss from soil, higher soil temperature and a shallower depth of frozen soil than those with a shallower snow cover (e.g. 2001–2002).

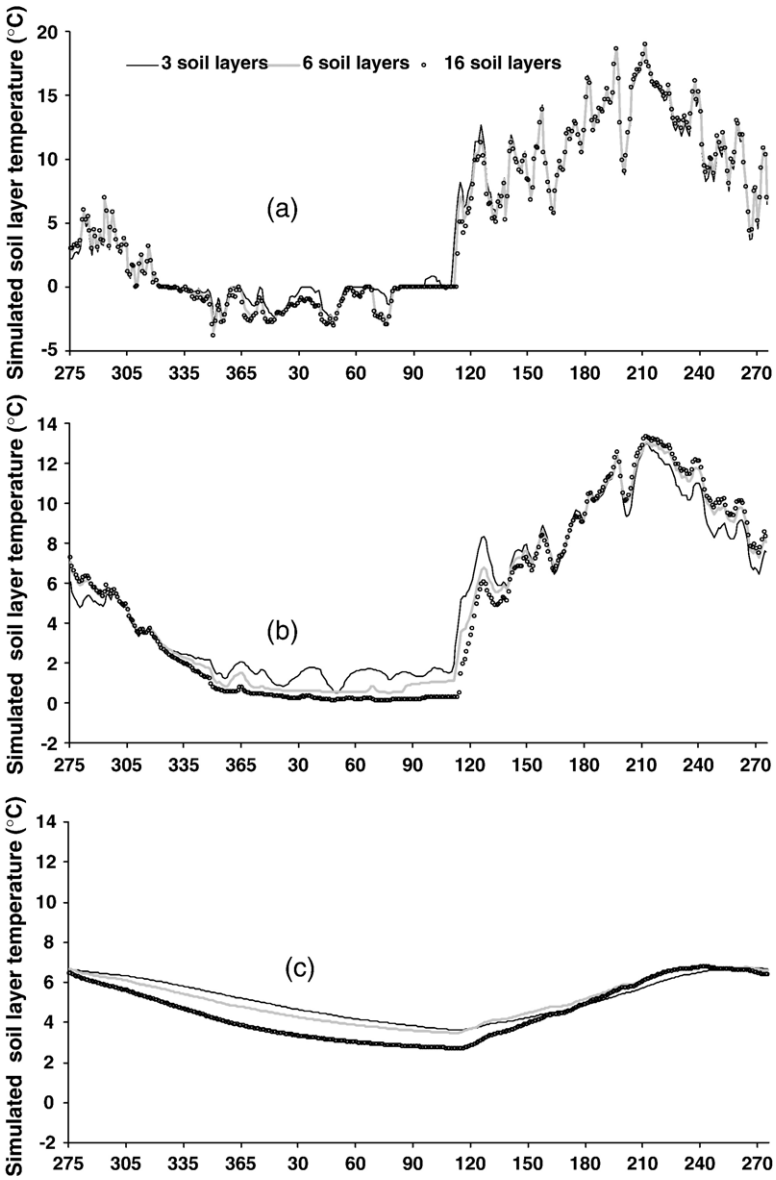

Fig. 6. Comparison of soil temperature simulation for 3 soil layers using 3 different soil layering resolutions. (a): for 0–0.1 m soil layer; (b): for 0.1–0.45 m soil layer; (c) for 0.45–4.15 m soil layer.

(3) The parameterizations of snow layer depth and the threshold snow depth for snow cover fraction had large effects on the snow simulations during snow melt, but little effect during the non-melt period. As a result, they affected the annual snow cover duration, but not the seasonally-averaged snow depth.

(4) The soil temperature simulations in the upper soil layers (e.g. above the 1 m soil depth) were affected by the depths of the water table and total soil column, but their effects were only significant below certain threshold values. The inclusion of a soil organic layer was important for soil temperature simulation, while the inclusion of unfrozen water in frozen soil had little effect at this site.

(5) Model testing with different soil layering resolutions showed that a 3-layer model configuration was too coarse to accurately simulate the soil thermal regime. A 6-layer resolution generated comparable results with a 16-layer resolution in

upper soil layers (0.65 m). Higher soil resolution was required to accurately simulate the deeper soil temperatures.

Our results indicate that soil temperature responses to future climate change will likely be complicated by the impact of climate change on snow cover, water table depth, and soil organic layer properties. Simulation schemes that could dynamically trace the changes of those variables and their interactions are highly desirable for future climate change impact assessments.

Acknowledgement

This study was supported by the "Reducing Canada's Vulnerability to Climate Change" Program of Earth Sciences Sector, Natural Resources Canada. We thank the observation team for the Southern Old Aspen site of BOREAS, BERMS and Fluxnet-Canada projects. We also thank the staff of the Fluxnet-Canada Data Information System, who made the data readily available. Funding for the field measurements was provided by Climate Research Branch of the Meteorological Service of Canada, the Canadian Forest Service, Parks Canada, the Action Plan 2000 on Climate Change, the Program of Energy Research and Development, the Climate Change Action Fund, the Natural Sciences and Engineering Research Council of Canada, the Canadian Foundation for Climate and Atmospheric Science, BIOCAP Canada and the USA National Aeronautics and Space Administration. The comments from Ian Olthof, Xiaolu Zhou and the two anonymous reviewers greatly improved the manuscript.

References

Amthor, J.S., Chen, J.M., Clein, J.S., Frolking, S.E., Goulden, M.L., Grant, R.F., Kimball, J.S., King, A.W., McGuire, A.D., Nikolov, N.T., Potter, C.S., Wang, S.S., Wofsy, S.C., 2001. Boreal forest CO_2 exchange and evapotranspiration predicted by nine ecosystem process models: intermodel comparisons and relationships to field experiments. J. Geophys. Res. Atmos. 106, 33623–33648.

Anderson, E.A., 1976. A point energy and mass balance model of snow cover, NOAA Technical Report NWS 19. US Department of Commerce, Silver Spring, MD. 150 pp.

Anderson, D., Nerbas, T., 2000. TE-1 SSA soil lab data. In: Newcomer, J., Landis, D., Conrad, S., Curd, S., Huemmrich, K., Knapp, D., Morrell, A., Nickeson, J., Papagno, A., Rinker, D., Strub, R., Twine, T., Hall, F., Sellers, P. (Eds.), Collected Data of The Boreal Ecosystem-Atmosphere Study. NASA. CD-ROM.

Auer, A.H., 1974. The rain versus snow threshold temperatures. Weatherwise 27, 67.

Barr, A.G., van der Kamp, G., Schmidt, R., Black, T.A., 2000. Monitoring the moisture balance of a boreal aspen forest using a deep groundwater piezometer. Agr. Forest Meteorol. 102, 13–24.

Barr, A.G., Black, T.A., Hogg, E.H., Kljun, N., Morgenstern, K., Nesic, Z., 2004. Inter-annual variability in the leaf area index of a boreal aspen-hazelnut forest in relation to net ecosystem production. Agr. Forest Meteorol. 126, 237–255.

Bartlett, P.A., MacKay, M.D., Verseghy, D.L., 2006. Modified snow algorithms in the Canadian land surface scheme: model runs and sensitivity analysis at three boreal forest stands. Atmosphere-Ocean 44, 207–222.

Betts, R.A., 2000. Offset of the potential carbon sink from boreal forestation by decreases in surface albedo. Nature 408, 187–190.

Bhatti, J.S., Fleming, R.L., Foster, N.W., Meng, F.-R., Bourque, C.P.A., Arp, P.A., 2000. Simulations of pre-and post-harvest soil temperature, soil moisture, and snowpack for jack pine: comparison with field observations. For. Ecol. Manag. 138, 413–426.

Black, T.A., den Hartog, G., Neumann, H.H., et al., 1996. Annual cycles of water vapor and carbon dioxide fluxes in and above a boreal aspen forest. Glob. Chang. Biol. 2, 219–229.

Black, T.A., Gaumont-Guay, D., Jassal, R.S., Amiro, B., Jarvis, P.J., Gower, T., Kelliher, F., Dunn, A., Wofsy, S., 2005. Measurement of CO_2 exchange between boreal forest and the atmosphere. In: Griffiths, H., Jarvis, P.J. (Eds.), The Carbon Balance of Terrestrial Biomes. Garland Science/BIOS Scientific Publishers, Oxford, pp. 120–141.

Celia, M.A., Bouloutas, E.T., Zarba, R.L., 1990. A general mass-conservative numerical solution for the unsaturated flow equation. Water Resour. Res. 26 (7), 1483–1496.

Clapp, R.B., Hornberger, G.M., 1978. Empirical equations for some soil hydraulic properties. Water Resour. Res. 14, 601–604.

Cox, P.M., Betts, R.A., Bunton, C.B., Essery, R.L.H., Rowntree, P.R., Smith, J., 1999. The impact of new land surface physics on the GCM simulation of climate and climate sensitivity. Clim. Dyn. 15, 183–203.

Essery, R., Etchevers, P., 2004. Parameter sensitivity in simulations of snowmelt. J. Geophys. Res. 109, D20111. doi:10.1029/2004JD005036.

Essery, R., Pomeroy, J., Parviainen, J., Storck, P., 2003. Sublimation of snow form coniferous forests in a climate model. J. Clim. 16, 1855–1864.

Foley, J.A., Kucharik, C.J., Polzin, D., 2005. Integrated Biosphere Simulator Model (IBIS), Version 2.5. Model product. Available on-line [http://daac.ornl.gov] from Oak Ridge National Laboratory Distributed Active Archive Center, Oak Ridge, Tennessee, U.S.A.

Goulden, M.L., et al., 1998. Sensitivity of boreal forest carbon balance to soil thaw. Science 279, 214–217.

Griffis, T.J., Black, T.A., Morgenstern, K., Barr, A.G., Nesic, Z., Drewitt, G.B., Gaumont-Guay, D., McCaughey, J.H., 2003. Ecophysiological controls on the carbon balances of three southern boreal forests. Agr. Forest Meteorol. 117, 53–71.

Groffman, P.M., Driscoll, C.T., Fahey, T.J., Hardy, J.P., Fitzhugh, R.D., Tierney, G.L., 2001. Colder soils in a warmer world: A snow manipulation study in a northern hardwood forest ecosystem. Biogeochemistry 56, 135–150.

Gusev, Y.M., Nasonova, O.N., 2003. The simulation of heat and water exchange in the boreal spruce forest by the land-surface model SWAP. J. Hydrol. 280, 162–191.

Johansen, O., 1975. Thermal conductivity of soils, Ph.D. thesis, Univ. of Trondheim, Trondheim, Norway.

Kongoli, C.E., Bland, W.L., 2000. Long-term snow depth simulations using a modified atmosphere-land exchange model. Agr. Forest Meteorol. 104, 273–287.

Lee, J., Pielke, R.A., 1992. Estimating the soil surface specific humidity. J. Appl. Meteorol. 31, 480–484.

Letts, M.G., Roulet, N.T., Comer, N.T., Skarupa, M.R., Verseghy, D.L., 2000. Parametrization of peatland hydraulic properties for the Canadian Land Surface Scheme. Atmosphere-Ocean 38 (1), 141–160.

Levine, E.R., Knox, R.G., 1997. Modelling soil temperature and snow dynamics in northern forests. J. Geophys. Res. 102 (D24), 29407–29416.

Li, X., Koike, T., 2003. Frozen soil parameterization in SiB2 and its validation with GAME-Tibet observations. Cold Reg. Sci. Technol. 36, 165–182.

Ling, F., Zhang, T., 2004. A numerical model for surface energy balance and thermal regime of the active layer and permafrost containing unfrozen water. Cold Reg. Sci. Technol. 38, 1–15.

Loth, B., Graf, H.F., 1998. Modeling the snow cover in climate studies: 2. Sensitivity to internal snow parameters and interface processes. J. Geophys. Res. 103 (D10), 11329–11340.

Luo, L., Robock, A., Vinnikov, K.Y., et al., 2003. Effects of frozen soil on soil temperature, spring infiltration, and runoff: results from the PILPS 2(d) experiment at Valdai, Russia, J. Hydrometeorol. 4, 334–351.

McCarthy, J.J., Canziani, O.F., Leary, N.A., Dokken, D.J., White, K.S. (Eds.), 2001. Climate Change 2001: Impacts, Adaptation and Vulnerability, Contribution of Working Group II to the Third Assessment Report of the Intergovernmental Panel on Climate Change (IPCC). Cambridge Univ. Press, New York. 1000pp.

Mellor, M., 1977. Engineering properties of snow. J. Glaciol. 19, 15–66.

Nijssen, B., et al., 2003. Simulation of high latitude hydrological processes in the Torne-Kalix basin: PILPS Phase 2(e). Glob. Planet. Change 38, 31–53.

Niu, G.Y., Yang, Z.L., 2006. Effects of frozen soil on snowmelt runoff and soil water storage at a continental scale. J. Hydrometeorol. 7, 937–952.

Ogée, J., Brunet, Y., 2001. A forest floor model for heat and moisture including a litter layer. J. Hydrol. 255, 212–233.

Pilon, C.E., Côté, B., Fyles, J.W., 1994. Effect of snow removal on leaf water potential, soil moisture, leaf and soil nutrient status and leaf peroxidase activity of sugar maple. Plant soil 162, 81–88.

Schlesinger, W.H., 1991. Biogeochemistry: An analysis of global change. Academic, San Diego, Calif.

Sellers, P.J., Hall, F.G., Kelly, R.D., et al., 1997. BOREAS in 1997: experiment overview, scientific results, and future directions. J. Geophys. Res. 102, 28731–28769.

Shewchuk, S.R., 1997. Surface mesonet for BOREAS. J. Geophys. Res. 102 (D24), 29077–29082.

Shewchuk, S.R., 2000. Atmospheric sciences infrastructure core measurements for BOREAS (AFM-07). In: Newcomer, J., Landis, D., Conrad, S., Curd, S., Huemmrich, K., Knapp, D., Morrell, A., Nickeson, J., Papagno, A., Rinker, D., Strub, R., Twine, T., Hall, F., Sellers, P. (Eds.), Collected Data of The Boreal Ecosystem-Atmosphere Study. NASA, CD-ROM.

Slater, A.G., Schlosser, C.A., Desborough, C.E., et al., 2001. The representation of snow in land surface schemes: results from PILPS 2(d). J. Hyhrometorol. 2, 7–25.

Stähli, M., Gustafsson, D., 2006. Long-term investigations of the snow cover in a subalpine semi-forested catchment. Hydrol. Process. 20, 411–428.

Sui, J., Koehler, G., 2001. Rain-on-snow induced flood events in Southern Germany. J. Hydrol. 252, 205–220.

Talbot, C.A., Ogden, F.L., Orb, D., 2004. Comment on "Layer averaged Richards' equation with lateral flow" by Praveen Kumar. Adv. Water Resour. 27 (10), 1041–1042.

Verseghy, D.L., 1991. CLASS — a Canadian land surface scheme for GCMs. I. Soil model. Int. J. Climatol. 11, 111–113.

Viterbo, P., Betts, A.K., 1999. Impact on ECMWF forecasts of changes to the albedo of the boreal forests in the presence of snow. J. Geophys. Res. 104, 27803–27810.

Wang, S., 2005. Dynamics of surface albedo of a boreal forest and its simulation. Ecol. Model. 183 (4), 477–494.

Wang, S., submitted for publication. Simulation of evapotranspiration and its response to plant water and CO2 transfer dynamics. J. Hydrometeorol.

Wang, S., Grant, R.F., Verseghy, D.L., Black, T.A., 2001. Modelling plant carbon and nitrogen dynamics of a boreal aspen forest in CLASS — the Canadian Land Surface Scheme. Ecol. Model. 142, 135–155.

Wang, S., Grant, R.F., Verseghy, D.L., Black, T.A., 2002a. Modelling carbon-coupled energy and water dynamics of a boreal aspen forest in a General Circulation Model land surface scheme. Int. J. Climatol. 22, 1249–1265.

Wang, S., Grant, R.F., Verseghy, D.L., Black, T.A., 2002b. Modelling carbon dynamics of boreal forest ecosystems using the Canadian Land Surface Scheme. Clim. Change. 55, 451–477.

Wang, S., Zhang, Y., Trishchenko, A., 2004. Ecological assimilation of land and climate observations — the EALCO model. Eos. Trans. AGU 85 (17) Joint Assembly Suppl., Abstract GC23A-11, JA146.

Wang, S., Trishchenko, A.P., Sun, X., 2007. Simulation of canopy radiation transfer and surface albedo in the EALCO model. Clim. Dynam. doi:10.1007/s00382-007-0252-y.

Whittaker, R.H., Likins, G.E., 1975. Primary production of the biosphere. Springer-Verlag, New York.

Winston, G.C., Sundquist, E.T., Stephens, B.B., Trumbore, S.E., 1997. Winter CO_2 fluxes in a boreal forest. J. Geophys. Res. 102 (D24), 28795–28804.

Yang, Z.L., Niu, G.Y., 2003. The versatile integrator of surface and atmosphere processes, Part 1. Model description. Glob. Planet. Change. 38, 175–189.

Yin, X., Arp, P.A., 1993. Predicting forest soil temperatures from monthly air temperature and precipitation records. Can. J. For. Res. 23, 2521–2536.